

# Nonlinear properties of bismuth whisker crystals under phonon generation conditions

Yu. A. Bogod, D. V. Gitsu, and A. D. Grozav

*Physicotechnical Institute of Low Temperatures, Ukrainian Academy of Sciences; Institute of Applied Physics, Moldavian Academy of Sciences*

(Submitted 29 October 1982)

Zh. Eksp. Teor. Fiz. **84**, 2194–2205 (June 1983)

The stationary current-voltage characteristics, the dynamics of transition to nonlinear conditions, and the “aftersound,” and nonreciprocity effects of bismuth single crystals are studied under conditions of counterdrift of electrons and holes. On the basis of the data obtained and of an analysis of the phonon kinetic equation it is concluded that the decisive mechanism of nonequilibrium phonon stabilization under the conditions considered is nonlinear phonon-phonon interaction. The density of the nonequilibrium phonons is shown to be a nonmonotonic function of the current density and to have a maximum at  $j \approx 3 \cdot 10^4$  A/cm<sup>2</sup>. This result is attributed to the increased probability of the three-phonon processes that cause departure of nonequilibrium phonons from the region of “overheating” caused by the generation. The nonreciprocity effect is ascribed to the various degrees of damping of the generated phonons at the ends of the specimen. It is suggested that this phenomenon can be used to record the generation of various acoustic modes.

PACS numbers: 63.20.Dj, 63.20.Hp, 61.55.Fe

## INTRODUCTION

In 1962, studying the magnetoresistance of bismuth in strong crossed electric and magnetic fields, Esaki observed that if the condition  $cE/Hs > 1 (\Omega\tau = eH\tau/m^*c \gg 1)$  is satisfied, the magnetoresistance decreases<sup>1</sup> ( $E$  and  $H$  are the electric and magnetic field strengths,  $s$  is the speed of sound, and  $m^*$  is the cyclotron mass of the carriers). The effect observed is due to phonon generation by electrons and holes that drift with supersonic velocity in a plane perpendicular to the electric field.

A specific feature of the Esaki effect is the bipolar drift of the carriers in the  $\mathbf{E} \times \mathbf{H}$  direction.<sup>2</sup> In the absence of a magnetic field, the electrons and holes drift in opposite directions. For this reason, the absorption coefficient of sound in bismuth, under the conditions  $\mathbf{E} \parallel \mathbf{E}_\sim$  and  $ql \ll 1$ , does not depend on the carrier drift velocity  $v_d$  (Ref. 3) ( $\mathbf{E}_\sim$  is the alternating field of the sound wave,  $q$  is the wave vector of the sound,  $l$  is the mean free path of the carriers); in other words, amplification of sound turns out to be impossible at  $v_d > s$ . Nonetheless, even in this situation, one can obtain on the current-voltage characteristic (CVC) the kink due to the averaging of the terms  $e(\langle n_- v_-^n \rangle + \langle h_- v_-^h \rangle)$  that are nonlinear in the electric field in the expression for the current ( $n_-$  and  $h_-$  are the nonequilibrium densities of the electrons and holes and  $v_-^{n,h}$  are the carrier velocities in the alternating field of the wave). The physical picture of the phenomenon is illustrated by the vector diagram in which the constant difference currents, ohmic and acoustoelectric, are summed for the electrons and holes:

$$\left. \begin{array}{l} \xrightarrow{v_{dn}^{ohm}} + \xleftarrow{v_{dn}^a} = \xrightarrow{v_{dn}^c} \\ \xleftarrow{v_{dh}^{ohm}} + \xrightarrow{v_{dh}^a} = \xleftarrow{v_{dh}^c} \end{array} \right\} \xrightarrow{j^c} = \xrightarrow{j_n^c} + \xrightarrow{j_h^c}$$

Here  $v_{di}^{ohm}$  and  $v_{di}^a$  are the ohmic and acoustoelectric drift velocities, and  $j^c$  is the total current through the sample.

Preliminary data on the observation of nonlinearity on the CVC of bismuth in the absence of an external magnetic field, a nonlinearity due to Čerenkov generation of the phonons, is contained in Ref. 4, where the objects of the investigations were chosen to be micron-size single crystals, whose advantages in similar experiments are undisputed. In the present study, the nonlinear properties of whisker single crystals of bismuth in the phonon generation regime have been investigated in detail: we investigated a stationary CVC, the dynamics of the transition into the nonlinear regime, the effects of “aftersound” and of nonreciprocity. The “aftersound” effect consists in the fact that when the external electric field, whose value corresponds to the supersonic drift of the carriers, is abruptly turned off there is registered on the sample a residual potential difference, due to dragging of the carriers by the previously excited nonequilibrium phonons. The nonreciprocity effect consists in nonreproducibility of the linear section of the CVC when the drift velocity is reversed.

## MEASUREMENT PROCEDURE, SAMPLES

The experiments were performed on cylindrical single crystals in glass insulation, obtained by casting from the liquid phase by the Ulitovskii method.<sup>5</sup> The cylinder axis made an angle  $19.5^\circ$  with the  $C_1$  direction in the bisector-trigonal plane  $C_1C_3$ . The samples were mounted on substrates of foil-clad paper-based laminate. The current and potential leads, in the form of coaxial cables, were connected with gallium solder or with Wood's alloy. The solder was deposited on the non-etched parts of the substrate, between which the sample was placed. The glass (pyrex) shell was not removed in the measurements. The characteristics of the samples and the results of the measurements made on them in the present study are listed in Table I.

Regardless of the type of solder, identical results were obtained for samples with close physical parameters. The

TABLE I.

Sample	Diameter, $10^{-4}$ cm	Length, cm	$R_{300}/R_{4.2}$ *
Bi-3B3	3.1	0.284	14.6
Bi-3B4	3.1	0.624	15.3
Bi-3B5	3.1	0.357	16.3
Bi-3B6	3.1	0.324	19.0
Bi-3B8	3.1	0.468	22.8
Bi-3B8A			
Bi-3B8B			
Bi-3B9	3.1	0.499	24.3
Bi-3B10	3.1	0.637	24.4
Bi-3B11	3.1	0.690	24.5
Bi-3B13	3.1	0.376	27.4

\*Measured with direct current.

conclusion that the nonlinear CVC is a manifestation of the properties of the material and not of the electric contacts can be drawn not only by changing the solder, but also by comparing the results of measurements made on samples of substantially different length with identical ratio of the ohmic resistances at room and helium temperatures  $R_{300}/R_{4.2}$ .

In the course of the experiments it was noted that after passing a direct current  $j > 5 \cdot 10^5$  A/cm<sup>2</sup> through sufficiently high-grade samples, the linear resistance measured at helium temperature increased irreversibly and accordingly the field  $E_c$  of the transition into the nonlinear regime increased.

This circumstance was used subsequently to obtain samples of various quality and identical geometrical parameters (see Table I, samples Bi-3B8, Bi-3B8A, and Bi-3B8B).

The CVC were measured by the usual pulse technique. The pulse repetition frequency was 40–100 Hz and the duration 1–10  $\mu$ sec. The source of the rectangular pulses was a commercial G5–27A generator, which ensured a signal rise time of 60 nsec to a matched load. Signals from the sample and from a standard resistor  $R_N = 50\Omega$  were recorded on the time sweep of an S8-2 oscilloscope.

In the study of the stationary CVC, the optimal choice of the gating time was determined, on the one hand, by the relaxation to the nonlinear regime, and on the other by the heating of the sample. To fix the latter, we used the circumstance that for a given value of  $E$  the nonlinear resistivity  $\rho' = E/j$  decreases with increasing temperature (Fig. 1). The diagram in the inset of Fig. 1 shows the dynamics of the heating in the phonon generation regime (the arrow  $OO_1$ ), the transition into the linear regime as a result of heating (the arrow  $O_1O_2$ ), and the increase of the resistance with temperature in the linear regime (the arrow  $O_2O_3$ ). The corresponding segments of the dynamic CVC are shown in Fig. 2 ( $AB$ ,  $A'B'$ , and  $B'C$ ).

Whereas the increase of the resistance as the result of generation of phonons in a given sample at a given temperature is determined by the strength of the electric field and is a threshold effect, the dynamics of the heating, as expected, depends also on the duration of the electric signal: the oscillogram segments corresponding to heating shift gradually with increasing electric field towards the start of the pulse. Understandably, the possibility of studying a stationary CVC in the generation regime is limited by the condition  $\tau_b \leq \tau_s$ , where  $\tau_b$  is the time of relaxation into the nonlinear

regime and  $\tau_s$  is the time during which the sample preserves the temperature of the thermostat or the interval during which the sample resistance remains constant when it is heated with electric current.

It is known that under stationary conditions liquid helium ensures heat dissipation at a power dissipation  $\approx 1$  W/cm<sup>2</sup>. Under the conditions  $j \leq 0.2 \times 10^5$  A/cm<sup>2</sup> and  $E \leq 0.4$  V/cm (see Fig. 2), on samples of diameter  $\sim 3 \mu$ m, the heat dissipation is approximately 0.6 W/cm<sup>2</sup>. Thus, according to the estimate, an increase of the resistance in the vicinity of the  $E_c$  (i.e., the transition into the generation regime) can be observed under stationary conditions, as was indeed confirmed in experiment. The glass insulation does not play a significant role here, since pyrex several microns thick is transparent to ultrasonic oscillations of frequency  $\sim 10^{11}$  Hz corresponding to the helium temperature region.<sup>6</sup> At  $E \approx 5.0, 2.3,$  and  $1.5$  V/cm (Fig. 2), the value of  $\tau_s$  in samples of the type Bi3-B9 was approximately 1, 4, and 10  $\mu$ sec, respectively.

## RESULTS OF EXPERIMENTS

1. A typical stationary CVC at helium temperature is shown in Fig. 2 (dark circles). It can be seen that at  $E > E_c$  the CVC is not linear, and the current saturation increases

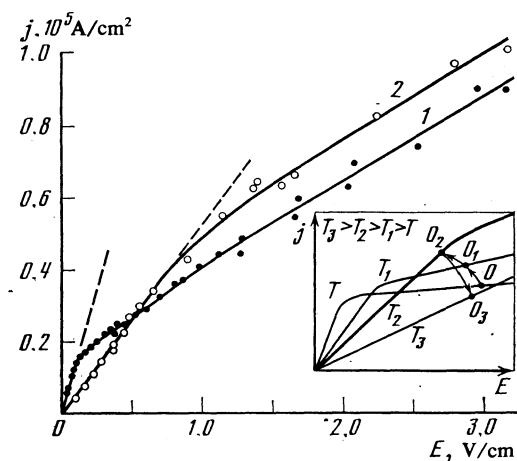


FIG. 1. CVC of sample Bi-3B5 at temperatures 4.2 K (curve 1) and 14.4 K (curve 2). The diagram in the inset shows how the dynamic sections of the CVC are formed when the sample is heated with electric current.

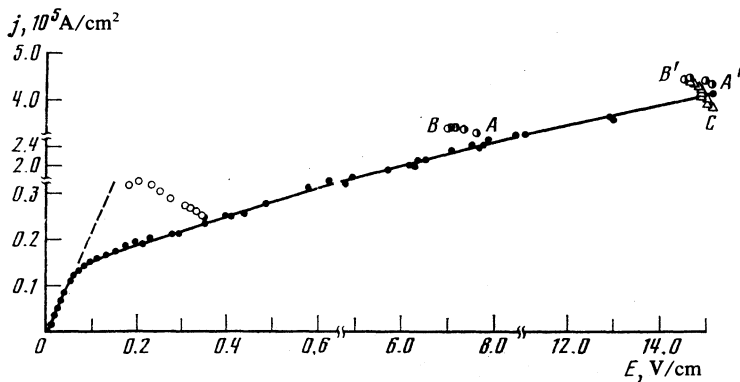


FIG. 2. Sample Bi-3B9,  $T = 4.2$  K. ●) Stationary CVC; ○) dynamic CVC on going into the generation regime; ○) sections of dynamic CVC in the course of heating in the generation regime; △) section of dynamic CVC when heated in the linear regime.

with increasing electric field intensity. Near  $E \approx 0.6$  V/cm, an increase of the derivative  $\partial j / \partial E$  is observed for all the samples (for details see below). When the stationary CVC is measured with direct and pulsed current the linear section of the CVC was not reproducible when the current was reversed—the non-reciprocity effect. Figure 3 shows the dependence of the nonreciprocity  $\Delta E$  on the current density on the stationary CVC obtained with direct current, with a resolution larger by three orders of magnitude than in the pulsed procedure. The inset shows a fragment of the  $\Delta E(j)$  plot for the sample Bi-3B3. If the nonreciprocity effect is regarded as a criterion for the transition into the nonlinear regime, the point where the CVC begins to be non-ohmic corresponds to values  $j \approx (3 - 4) \cdot 10^3$  A/cm<sup>2</sup> and  $E \approx (2 - 3) \cdot 10^{-2}$  V/cm.

2. The dynamic CVC, on going in the generation regime into the state  $j \approx 0.24 \cdot 10^5$  A/cm<sup>2</sup> and  $E \approx 0.35$  V/cm, is shown in Fig. 2 by the light circles (gating every 0.1  $\mu$ sec). Since the slope of the leading front of the pulse is large enough (see above), the relaxation time  $\tau_b$  on going into the nonlinear regime was measured from the time of the start of the input signal to the saturation of  $E$  (or  $j$ ). The dependence of the time of relaxation to the nonlinear regime on the current density, obtained for the sample Bi-3B11 with the aid of voltage oscillograms, is shown in Fig. 4.

3. The aftersound effects observed at  $E > E_c$  was measured by a null method. It was observed that the amplitude  $E_p$  of the aftersound, and consequently the density of the nonequilibrium phonons in the sample, goes through a maximum, other conditions being equal, when the current and voltage increase (Fig. 5). The maximum of  $E_p$  is observed in

the same vicinity of  $j$  at  $E$  as the increase of the derivative  $\partial j / \partial E$  in the stationary CVC (inset in Fig. 5).

The time  $\tau_m$  from the instant when the voltage drop across the sample goes through zero to the peak of the aftersound, which corresponds physically to the phonon-electron relaxation time  $\tau_{pe}$ , changes in step with  $E_p$ , going through a maximum in the same region of  $j$  and  $E$  (Fig. 5). According to our present data,  $\tau_{pe} \lesssim 0.2$   $\mu$ sec for the sample Bi-3B4.

The fact that aftersound was observed in the nonlinear regime is evidence of the existence of a directed flow of non-equilibrium phonons, proving thereby the decisive contribution to the effect of phonon generation of carriers of one type—electrons or holes, which drift opposite to each other. The orientation of the investigated whisker crystals was such that without allowance for the boundary effect the drift current is due mainly to electrons which, apparently, produce in fact the phonon flux. If this is so, the sign of the aftersound signal makes it possible to state that the decisive factor is the dragging of the electrons and not of the holes by the phonons. To observe dragging of holes by phonons, an experiment was performed whose idea consisted in the following. A doubly rectangular pulses, shown schematically in Fig. 6b, applied to the sample. Initially the conditions  $E_1 \ll E_c$  and  $E_1 + E_2 > E_c$  were satisfied. It is clear that when oscillograms are taken of the response of the sample to the external signal, there should be observed on the trailing edge of the upper pulse the aftersound effect referred to above. With increasing  $E_1$ , the drift velocity of the electrons, which corresponds to the lower part of the signal, increases and becomes close to the speed of sound at  $E_1 \approx E_c$ . Therefore the phonons flux produced by the electrons under the field  $E_1 + E_2$

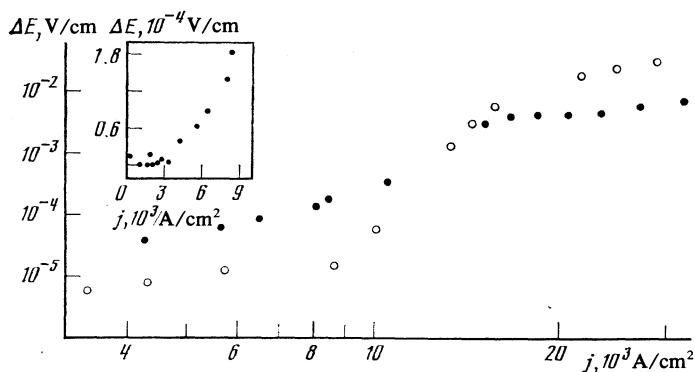


FIG. 3. Dependence of the nonreciprocity  $\Delta E$  on the current density  $j$  on the stationary CVC, obtained with direct current: ●) Bi-3B3, ○) Bi-3B6. The inset shows the fragment of the dependence of  $\Delta E$  on  $j$  for sample Bi-3B3.

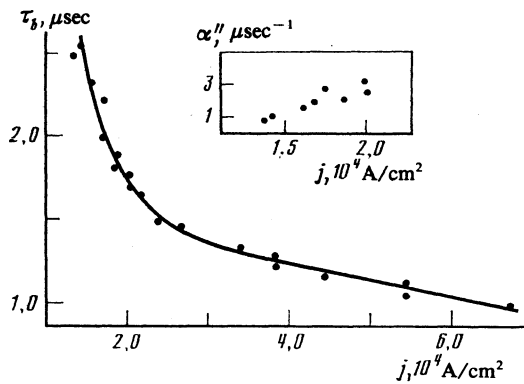


FIG. 4. Dependence of the time  $\tau_b$  of relaxation to the nonlinear regime on the current density  $j$ , for the sample Bi-3B11 at  $T = 4.2$  K. The inset shows the dependence of the coefficient  $\alpha''$  on  $j$  for the same sample [see Eq. (5)].

leads only to a change in the distribution of the holes in the sample, leaving unchanged the distribution of the electrons that drift with velocity  $v_d \approx s$ . Thus, the aftersound effect observed on the trailing edge of the upper part of the signal from the sample should reverse sign, as is indeed observed in experiment (Fig. 6, b-d). When  $E_1 > E_c$ , the picture is supplemented by aftersound having the usual electronic sign on the trailing edge of the lower part of the signal from the sample (Fig. 6d).

4. By applying to the sample two successive identical pulses separated by an adjustable time interval it is possible to study the damping of the nonequilibrium phonons that remain in the sample after turning off the external electric field corresponding to the supersonic drift of the carriers.

Let us examine the schematic form of the dynamic CVC in the  $dc$  regime (Fig. 7, line OAB on inset d), assuming that the growth time of the driving pulses  $t_1 \rightarrow 0$ . Each point of the

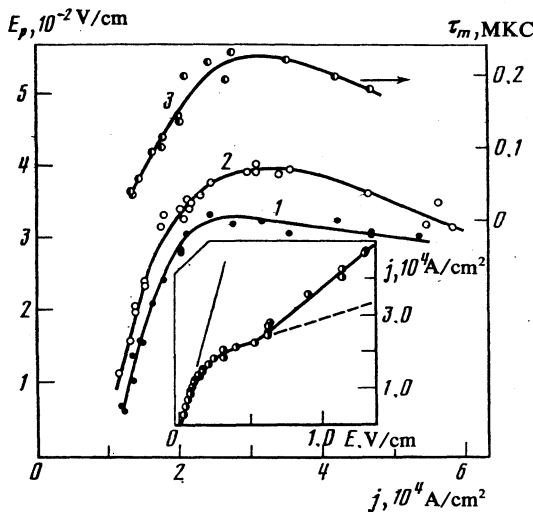


FIG. 5 Amplitude of the aftersound  $E_p$  (curves 1 and 2) and the time interval  $\tau_m$  from the instant of the passage of the sample voltage signal through zero to the peak of the aftersound (curve 3) vs the current density  $j$ . Samples: 1, 3—Bi-3B4; 2—Bi-3B10. For curve 3, the ordinate is on the right. Inset—stationary CVC of the sample Bi-3B4.

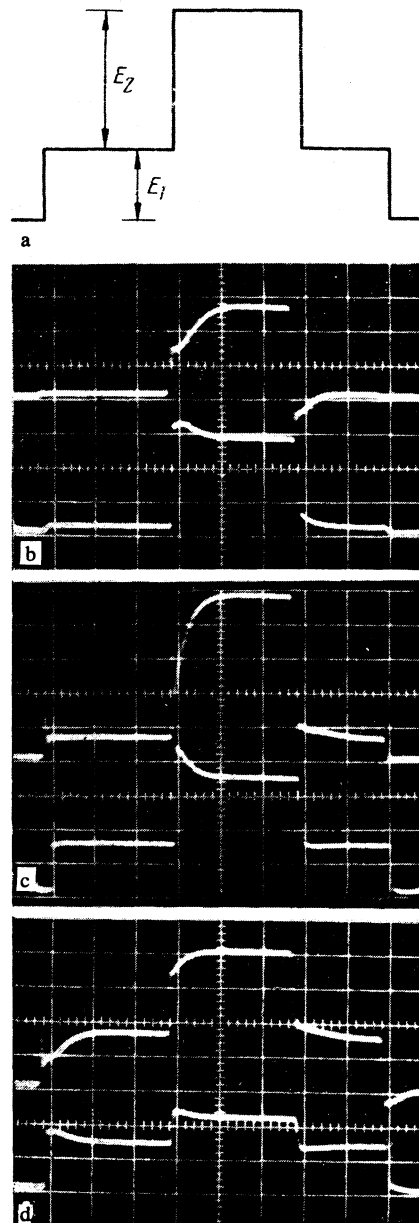


FIG. 6. Observation of electron and hole dragging by nonequilibrium phonons by the method of doubly rectangular pulses (a). Sample Bi-3B13  $T = 1.9$  K. Vertical scale: b, c— $0.25$  V/div ( $U$  and  $U_N$ ); d— $0.05$  V/div ( $U$  and  $U_N$ ). Horizontal scale— $1.0$  sec/div.

line  $AB$  of the given CVC can be set in correspondence with a definite density of the nonequilibrium phonons,  $N_i$ , which will be shown below to be proportional, at a constant drift velocity  $v_d \propto j$ , to the voltage difference<sup>1)</sup>  $U_i - U_0$ . Assume that at a certain time  $t_2$  after turning off the external field, a second pulse of the same amplitude  $J_0$  is applied to the sample. If at the instant when the second pulse is turned on the number of equilibrium phonons in the sample differs from zero, when the current reaches its maximum amplitude the electric field intensity in the sample reaches a certain value  $E_1$  corresponding to the density of the residual nonequilibrium phonons. Thus, by measuring the difference  $\Delta U$  of the initial response signals to the first and second pulses it is

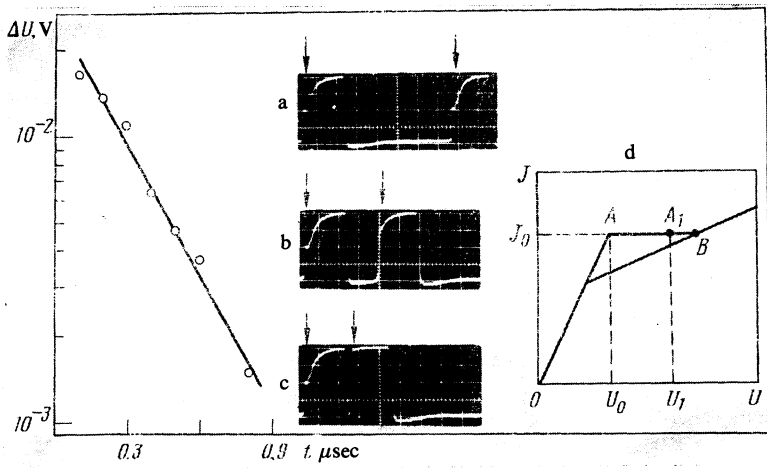


FIG. 7. Illustrating the study of the damping of nonequilibrium phonons by the method of two successive pulses: Dependence of the difference of the response signals  $\Delta U$  on the time interval between the trailing edge of the first pulse and the leading edge of the second pulse (sample Bi-3B4). In insets a-c are shown oscillograms illustrating the method of measuring the coefficient  $\beta_1$ ; the arrows indicate the points for which the value of  $\Delta U$  was determined. Inset d shows a schematic plot of the dynamic CVC in the given-current regime.

possible to obtain information on the damping of the nonequilibrium phonons. Naturally, this method leads to correct results at  $t_1 \ll \tau_b, \tau_p$ , where  $\tau_p$  is the relaxation time of the residual nonequilibrium phonons. The indicated inequality was satisfied in the present investigation). An additional source of errors are the measurements made not in the given-current regime. For this reason, in the present study the data concerning  $\Delta U(t) \propto N_q(t)$  were obtained at low values of  $E$ , when the ratio of the sample and load resistances was as small as possible. Figure 7 shows the difference between the response signal as a function of the distance between the trailing edge of the first pulse and the leading edge of the second, which is equivalent to the  $N_q(t)$  dependence. Compared with direct measurement of the aftersound effect, the method considered here has the advantage that the aftersound signal is a result of only phonon-electron interaction and consequently is in principle impossible to record with its aid the damping of phonons over times shorter than  $\tau_{pe}$ .

## DISCUSSION OF RESULTS

1. To process the stationary CVC it is natural to use the phenomenological model of Ref. 2, which is based on the concept of the acousto-emf  $E^a$ , which depends on the number of nonequilibrium phonons, and on the sound-generation coefficient  $\gamma$ ; they are connected by a relation similar to the Weinreich equation.<sup>7,2</sup> By including the acousto-emf  $E^a$  in the equation of motion for the drift velocity of the carriers we obtain, in the approximation of isotropic dispersion with identical parameters of the spectrum and of the scattering of the electrons  $n$  and of the holes  $h$ , an expression for the total current

$$j = \sigma E (1 - E^a/E), \quad (1)$$

where  $\sigma$  is the ohmic conductivity,  $E^a = E_n^a = E_h^a$ . In the vicinity of the point of transition into the nonlinear regime we have  $E^a/E \ll 1$ , and the specific electric power is  $W_{n,h} \approx \sigma E^2/2$ , so that

$$j \approx \sigma E (1 - \Gamma \sigma E / 2nes). \quad (2)$$

Here  $\Gamma = \gamma - \delta$ , where  $\delta$  is determined by non-electronic mechanisms of sound damping. At an arbitrary relation between  $E^a$  and  $E$  we have

$$E^a = E + \frac{nes}{\Gamma \sigma} \left[ 1 \pm \left( 1 + \frac{2\Gamma \sigma E}{nes} \right)^{1/2} \right]. \quad (3)$$

Inasmuch as in experiment we always have  $E^a/E < 1$ , it is necessary to use the minus sign in Eq. (3).

Substituting (3) in (1), assuming  $s = 10^5$  cm/sec, and using the values of  $J, \sigma$ , and  $E$  taken from experiment, we can plot the dependence of the effective generation coefficient  $\Gamma$  on the current density, which is proportional to the drift velocity  $v_d$ . The corresponding plots for the sample Bi-3B9, Bi-3B8, Bi-3B8A, and Bi-3B8B are shown in Fig. 8. As can be seen from the figure,  $\Gamma(j)$  is a nonmonotonic function whose maximum practically coincides with the maximum of the  $E_p(j)$  dependence, see Fig. 5. Since the decrease of the amplitude of the aftersound reflects a decrease of the density of the nonequilibrium phonons in the sample, it is natural to attribute to the same cause also the presence of a maximum on the  $\Gamma(j)$  curve.

As follows from (2), the condition for observing the non-linearity of the CVC is  $\Gamma \sigma E / 2nes \sim 1$ . Therefore the increase in the current density at which the inflection of the CVC is

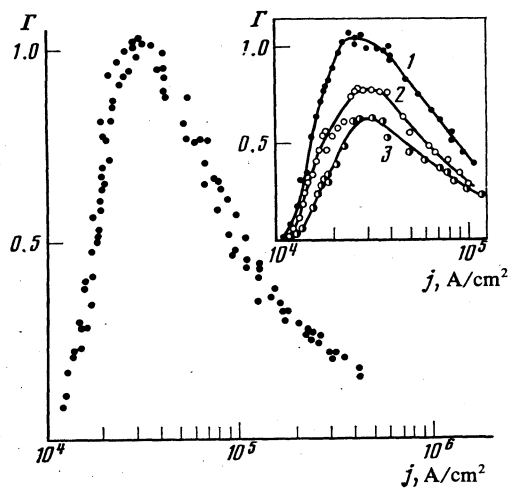


FIG. 8. Dependence of the effective generation coefficient  $\Gamma$  on the current density  $j$  for the sample Bi-3B9. Inset—the corresponding dependences for the samples Bi-3B8 (1), Bi-3B8A (2), and Bi-3B8B (3).

observed with increasing temperature is the consequence of the  $\Gamma(T)$  dependence connected with the damping of the nonequilibrium phonons by the normal ones, i.e., with the increase of the coefficient  $\delta$ .<sup>2</sup> From the definition of the acousto-emf and from Eq. (1) it follows that the voltage drop  $\Delta E$  across the sample in the case of current reversal can be the result of the difference in the damping of the nonequilibrium phonons at the end faces of the sample. In this case, the nonreciprocity  $\Delta E$  takes the form

$$\Delta E = \Delta E^a = \Delta \delta W / nes. \quad (4)$$

In the nonlinear regime, the specific power fed into the electron system increases with increasing current approximately in accord with the law  $W \propto j^2$ , and consequently, for  $\Delta \delta = \text{const}$  it is necessary to have  $\Delta E \propto j^2$ . As can be seen from Fig. 3, the nonreciprocity depends on the current density in accordance with a more complicated law, but follows a qualitative relation, namely, an increase in the power is always accompanied by an increase in the measured potential difference (we emphasize that the shape of the function  $\Delta E(j)$  is the same for all samples). To explain the results it is possible to advance, as an alternative, the hypothesis that  $\Delta \delta$  depends on the frequency of the generated phonons which, as will be shown below, can vary as a function of their density.

One other possibility of changing the phonon frequency is excitation of different acoustic modes with increasing drift velocity. In the latter case the plot of  $\Delta E(j)$  should have segments in which  $\Delta E \propto j^2$  and which are connected by a certain transition region corresponding to excitation of a new acoustic mode. A plot of  $\Delta E(j)$  shown in Fig. 3 has two segments with the  $\Delta E \propto j^2$  dependence. It can be assumed on this basis that the increase of the derivative  $\partial \log(\Delta E) / \partial \log j$  in the vicinity of  $j \approx 10^4 \text{ A/cm}^2$  and  $E \sim (7.9) \cdot 10^{-2} \text{ V/cm}$  is connected with the excitation of fast shear or longitudinal acoustic modes.

2. We shall assume that the change in the number of the nonequilibrium phonons in the sample at  $E > E_c$  is described by the law

$$\partial N_q / \partial t = \alpha'' N_q - \beta N_q^2 + C, \quad (5)$$

where

$$\alpha'' = \alpha - \alpha' - \delta' > 0, \quad C = \alpha'' N_{q0} - \beta N_{q0}^2 + \alpha_q'.$$

In expression (5) we used the following notation:  $\alpha$  is the growth rate of the phonons generated by the carriers that drift with supersonic velocity;  $\delta'$  is the decrement of the damping by the oppositely moving carrier;  $\gamma'$  is the decrement of non-electronic damping;  $\alpha_q'$  and  $\beta$  are coefficients that describe respectively the spontaneous generation of the phonons at  $v_d > s$  and the nonlinear phonon-phonon damping. The quantities  $\alpha$ ,  $\alpha'$ , and  $\beta$  (Ref. 8) are functions of the drift velocity;  $N_{q0}$  is the number of equilibrium phonons.

We assume also that in the stationary state the number of nonequilibrium phonons  $N_{qs}$  is much larger than that of the equilibrium ones, i.e.,

$$\alpha'' N_{qs}, \beta N_{qs}^2 \gg C, \quad N_{qs} \approx \alpha'' / \beta \gg N_{q0}.$$

The integral of Eq. (5) is the expression

$$N_q \approx e^{\alpha'' t} \left[ \frac{\beta}{\alpha''} (e^{\alpha'' t} - 1) + A^{-1} \right]^{-1} - A, \quad (6)$$

where

$$A = \frac{-\alpha'' + [(\alpha'')^2 + 4\beta C]^{1/2}}{2\beta} \approx \frac{C}{\alpha''} \approx N_{q0}.$$

According to (6), at

$$\frac{\beta}{\alpha''} (e^{\alpha'' t} - 1) < N_{q0}^{-1} \quad (7)$$

the number of phonons increases almost exponentially, and then, after the opposite inequality is reached, it tends to saturation. If the gain  $\alpha''$  increases with increasing drift velocity, the number of phonons should increase more rapidly and should reach earlier the saturation corresponding to the stationary state in the linear regime. This result correlates with the experimentally observed  $\tau_b(j)$  dependence. This circumstance allows us to conclude that the decisive mechanism of stabilization of the nonequilibrium phonons under the conditions considered is the nonlinear phonon-phonon interaction.

Qualitative information on the coefficient  $\alpha''$  can be obtained by using the proportionality of the acousto-emf to the arrival term in Eq. (5), i.e.,  $E^a \propto \alpha N_q$ . If we neglect the change of the current density during the pulse and recognize that when the inequality (7) is satisfied we have  $n_q \propto \exp(\alpha'' t)$ , it is easy to obtain from Eq. (1) and from experiment the  $\alpha''(j)$  dependence. The result is shown in Fig. 1, from which it follows that at  $j \lesssim 2 \cdot 10^4 \text{ A/cm}^2$  the coefficient  $\alpha''$  increases with increasing drift velocity. The change of the growth rate at large values of the current under the conditions of the present paper is meaningless, owing to the increasing experimental error. The character of the  $\tau_b(j)$  dependence, however, indicates that at  $j > 2 \cdot 10^4 \text{ A/cm}^2$  the value of  $\alpha''$  does at any rate not decrease.

Using the condition  $\exp(\alpha'' \tau_b) \sim N_{qs} / N_{q0}$ , we can obtain an estimate of the relative density of the nonequilibrium phonons. For the sample Bi-3811 at  $j \approx 2 \cdot 10^4 \text{ A/cm}^2$  we have  $N_{qs} / N_{q0} \approx 4 \cdot 10^2$ .

3. The decrease of the density of the nonequilibrium phonons, observed at  $j \gtrsim 3 \cdot 10^4 \text{ A/cm}^2$  experimentally with the aid of the aftersound effect, in conjunction with expressions (5) and (6), means a faster growth of the coefficient  $\beta$  relative to  $\alpha''$  (from which it follows, in particular, that the maximum of the function  $\Gamma(j)$  is due to the increase of the coefficient  $\delta$ ). The physical cause of the dependence of  $\beta$  on the drift velocity lies in the broadening of the Čerenkov radiation cone. According to theoretical calculations in Ref. 8, we have  $\beta \sim 1 - s/v_d$ . It appears that in thin samples the expansion of the radiation cone should lead to an additional increase of the coefficient  $\beta$ , due to the formation of opposing phonon streams when the phonons are reflected from the sample boundaries. It can be assumed that when  $n_{qs}$  increases phonons are transferred to the long-wave region of the spectrum (transfer over the spectrum is known to occur

in semiconductor crystals<sup>9</sup>). This is probably also the cause of the maximum on the  $\tau_m(j)$  curve which is similar to the plot of the density of the nonequilibrium phonons against the drift velocity.

We note that the possibility of describing the experimental results within the framework of the kinetic equation (5) and the nonequilibrium-flux recorded in the sample with the aid of the aftersound offer evidence that the decisive contribution to the measured effect is made by phonons with wave vector  $q \gg l^{-1}$  (Ref. 3).

4. If we start from the assumption that  $N_{qs} \gg N_{q0}$ , the damping of the nonequilibrium phonons when the external field is turned off can be described by Eq. (5), assuming  $C = 0$  and introducing in place of  $\alpha''$  the coefficient  $-\beta_1$  that describes the total linear absorption at  $v_d = 0$ . In this case the function  $N_q(t)$  takes the form

$$N_q = e^{-\beta_1 t} \left[ \frac{\beta}{\beta_1} (1 - e^{-\beta_1 t}) + N_{qs}^{-1} \right]^{-1}. \quad (8)$$

If  $N_{qs}$  is such that

$$\frac{\beta}{\beta_1} (1 - e^{-\beta_1 t}) \ll N_{qs}^{-1},$$

the damping of the nonequilibrium phonons with time is described by an exponential law. Comparing the foregoing with the experimental plot of  $\Delta U(t)$  in Fig. 7, which is equivalent to  $N_q(t)$ , we obtain for the damping decrement of the nonequilibrium phonons the value  $\beta_1 \approx 3.6 \cdot 10^6 \text{ sec}^{-1}$ .

## CONCLUSION

A distinguishing feature of the present study is the investigation of effects of phonon generation in a compensated object in the case of oppositely drifting electrons and holes. We have observed a nonreciprocity effect, namely nonreproducibility of the nonlinear section of the stationary CVC when the drift velocity changes direction; this effect is attributed to the different degree of damping of the generated phonons at the end faces of the sample. A hypothesis was advanced that it is possible to record generation of different acoustic modes with the aid of this phenomenon.

We measured the dependence of the relaxation time on the current density in the transition to the nonlinear regime. On the basis of the data obtained and of an analysis of the kinetic equation for the phonons, we have concluded that the decisive mechanism that stabilizes the nonequilibrium phonons under the conditions considered is nonlinear phonon-phonon interaction.

We have observed directly the dragging of electrons and holes by nonequilibrium phonons. We have shown that the density of the non-equilibrium phonons is a nonmonotonic function of the current density and has a maximum at  $j \approx 3 \cdot 10^4 \text{ A/cm}^2$ . This result correlates with the properties of the generation coefficient and is connected with the increase of the probability of three-phonon processes that cause the equilibrium phonons to leave the region overheated by the generation.

A method was proposed for studying the damping of nonequilibrium phonons in the given-current regime with the aid of two successive pulses with adjustable spacings between them.

The authors are grateful to R. G. Valeev for help with the experiment and A. I. Kopeliovich for a discussion of the results.

<sup>11</sup> In the given-voltage regime, the change of the current is accompanied by a change not only of the phonon density, but also of the coefficient that connects this density with the current density (see below).

<sup>1</sup> L. Esaki, Phys. Rev. Lett. 8, 4 (1962)

<sup>2</sup> Yu. A. Bogod, Fiz. Nizk. Temp. 8, 787 (1982) [Sov. J. Low Temp. Phys. 8, 393 (1982)].

<sup>3</sup> Yu. A. Bogod, ibid. 7, 662 (1981) [7, 326 (1981)]

<sup>4</sup> N. B. Brandt, D. V. Gitsu, A. M. Ioisher, B. P. Kotrubenko, and A. A. Nikolaeva, Prib. Tekh. Eksp. No. 3, 256 (1976).

<sup>5</sup> M. Pomerantz and R. J. von Gutfeld, Proc. 9th Internat. Conf. on Semicond. Phys. Moscow, 1968, Vol. 2, Nauka, 1969, p. 732.

<sup>6</sup> A. Weinreich, Phys. Rev. 107, 317 (1957).

<sup>7</sup> H. Ozaki and N. Mikoshiha, J. Phys. Soc. Jpn. 21, 2486 (1966).

<sup>8</sup> I. M. McFee, J. Appl. Phys. 34, 1548 (1963).

Translated by J. G. Adashko